Fuel 303 (2021) 121251

Contents lists available at ScienceDirect

Fuel

journal homepage: www.elsevier.com/locate/fuel

Full Length Article

Ignition delays of biodiesel-diesel blends: Investigations into the role of physical and chemical processes

Phuong X. Pham [a], Nam V.T. Pham [a], Thin V. Pham [b], Vu H. Nguyen [a,*], Kien T. Nguyen [a,*]

[a] Faculty of Vehicle & Energy Engineering , Le Quy Don Technical University, 236 Hoang Quoc Viet, Bac Tu Liem, Ha Noi 10000, Viet Nam
[b] Faculty of Physical and Chemical Engineering, Le Quy Don Technical University, 236 Hoang Quoc Viet, Bac Tu Liem, Ha Noi 10000, Viet Nam

ARTICLE INFO

Keywords:
Biodiesel
Chemical ignition delay
Physical ignition delay
Atomization
Evaporation

ABSTRACT

Overall ignition delay (ID_{over}) recorded in Compression-Ignition engines (CIEs) is caused by physical and chemical processes. Those processes lead to physical and chemical ignition delay times (ID_{phys} and ID_{chem}, respectively). ID_{over} could be understood as the sum of ID_{phys} and ID_{chem}, although some overlap could exist between them. Knowledge on diesel and biodiesel ignition delay times is quite mature, however, the role of physical and chemical processes on the times is not quite clear and this requires additional studies to further examine these important processes. This paper investigates the contribution of physical and chemical processes into ID_{phys}, ID_{chem}, and ID_{over} of a wide-range of biodiesels and their blends with fossil-diesel in CIEs. ID_{over} is measured here using a cooperative-fuel-research engine and a 6-cylinder engine. A shocktube is used to measure ID_{chem} while physical processes including atomization and evaporation are experimentally examined. It is found that size and distribution of drops derived from the atomization process of the fuels are somewhat similar while the evaporation rate of biodiesels is much slower compared to that of diesel and this could cause their longer ID_{phys}. ID_{chem} is characterised by chemical reactions that could be initiated at high temperature coefficient - HTC, negative temperature coefficient - NTC or low temperature coefficient – LTC regimes. ID_{chem} of fuels tested under HTC is identical while ID_{chem} under NTC and LTC regimes is determined by the fuel molecular structure. Compared to diesel, ID_{chem} of common biodiesels is shorter and this could be attributed to their faster rates of reactions under NTC and LTC; their ID_{phys} is longer and this is mainly due to their longer evaporation rate; but in overall, their ID_{over} is shorter.

1. Introduction

Ignition delay (ID), known as the first phase of combustion process occurring in compression ignition engines (CIEs), has crucially significant effects on CIEs' performance and pollutants. Controlling ID time could be a clue to improve engine efficiency and to decrease fuel consumption and exhaust emission [1]. For example, decreasing ID in an engine was found to be an effective approach to reduce NOx in modern CIEs [1]. Shorter ID of a fuel generally leads to longer combustion duration and lower peak in-cylinder pressure [2,3]. In the ID period of CIEs, the liquid undergoes complex physical and chemical processes toward the auto-ignition event and as such ID is well-known as an indicator of fuel auto-ignitability. The period is measured from the start of fuel injection (SOI) to the auto-ignition event or start of combustion (SOC). ID is attributed to physical and chemical processes which are occurring simultaneously under complex in-cylinder temperature and pressure conditions [2]. Physical processes mainly comprise of penetration, atomization, heating, vaporization, and mixing while chemical processes include preliminary exothermic chemical reactions [4].

In auto-ignition engines, the chemical processes are the pre-major-heat-releasing reactions leading to auto-ignition [5]. Generally, each chemical reaction occurs when a sufficient amount of energy to break the molecular bonds causing the reaction to take place, this energy is well-known as activation energy. Auto-ignition event is kinetically described by chemical reaction mechanism. Reactions could be occurred under different mechanism such as thermal ignition, chain branching reactions, oxidation of hydrogen and of carbon monoxide, and chain-thermal interactions [6]. Thermal ignition involves chemistry without chain branching and represents systems in which thermal feedback occurs. In complex chemically reacting systems like heat engines, the actual chemical mechanism consists of a large number of chain reactions or simultaneous and independent reactions and steps [5]. In such chains, the initiating reaction produces highly reactive intermediate species or

* Corresponding authors.
E-mail addresses: phuongpham@lqdtu.edu.vn (P.X. Pham), vunguyenhoang@lqdtu.edu.vn (V.H. Nguyen), kiennt@lqdtu.edu.vn (K.T. Nguyen).

https://doi.org/10.1016/j.fuel.2021.121251
Received 7 April 2021; Received in revised form 17 May 2021; Accepted 7 June 2021
Available online 7 July 2021

Nomenclature

ID	Ignition delay
ID_{phys}	Physical ignition delay
ID_{chem}	Chemical ignition delay
CIE	Compression ignition engine
CR	Compression ratio
CN	Cetane number
SOI	Start of injection
SOC	Start of combustion
HTC	High temperature coefficient
NTC	Negative temperature coefficient
LTC	Low temperature coefficient
CFR	Cooperative fuel research
DCA	Degree of crank angle
IQT	Ignition quality tester
BTDC	Before top dead centre
FAME	Fatty acid methyl esters
OR	Oxygen ratio
OFR	Oxygen fuel ratio
AFR	Air fuel ratio
λ	Air-fuel equivalence ratio
HRR	Heat release rate

radicals. This is followed by propagation and termination reactions. In those processes, there is a chain-branching reaction where the number of radicals is sufficiently rapidly increased. The reactions and steps could be occurred under high temperature coefficient – HTC, negative temperature coefficient – NTC or low temperature coefficient – LTC regimes [7–9]. HTC, NTC and LTC mechanisms are reported in details in [9]. The reader could also be directed to ref. [5] for further details on the auto-ignition chemistry terminologies (e.g. cool / hot flames, two-stage ignition, single-state ignition, and so on).

Studies on overall ID (ID_{over}) time in CIEs could be found in the literature. Those studies could be classified into two groups: (i) examining the influence of isolated physical or chemical process (e.g. atomization, evaporation, or reaction mechanism) on ID and (ii) directly exploring ID_{over} in engines. Good reviews on ID of diesel and biodiesel in engines are provided in refs [10–13]; a review on spray of biodiesels in CI engines can be found in [14]; and the reader is directed to [15] for information on biodiesel spray morphology, combustion and emission. However, ignition delay is a very complex phenomenon and the roles of physical and chemical processes on ID need to be further explored. This is particularly true with the advent of alternative fuels like biodiesels investigated in this current study. Our effort provided here aims to investigate the impact of important physical and chemical processes affecting the ID_{over} observed in CIEs fuelled with biodiesels having different molecular structures (see Table 2) and their blends with fossil diesel (D). This may link with current studies on chemical reaction kinetics (e.g. [9,16–18]), atomization (e.g. [14,19–21]), and evaporation (e.g. [19,22,23]) in the current literature to provide better knowledge on the influence of physical and chemical processes on ID of biodiesels and their blends.

Although combined studies on ID_{over}, physical and chemical ID are quite limited, some notable reports can be found in the literature. In the old days, ID in CIEs has been assumed to the sum of physical ID (ID_{phys}) and chemical ID (ID_{chem}) [24,25], $ID_{over} = ID_{phys} + ID_{chem}$. Although ID_{phys} and ID_{chem} are not consecutively occurring as there exist some overlap between these two periods. The arbitrary separation between ID_{phys} and ID_{chem} allows the chemical reaction kinetics to be distinguished from all the other factors that determine the physics of the fuel injection process [2]. In this context, ID_{phys} was understood as the time between the SOI (needle lift) and to the initial point where the mixture fraction and in-cylinder temperature conditions are reached for chemical reactions to begin, then, the ID_{chem} period will take place.

Numerically, ID time (τ) of a fuel can be computed using the well-known Arrhenius correlation as shown in Equation (1) [26]:

$$\tau = \boldsymbol{A}.\mathbf{p}^{-\boldsymbol{m}}.\boldsymbol{exp}\left(\frac{\boldsymbol{E_a}}{\boldsymbol{RT}}\right)\boldsymbol{\varphi}^{-\boldsymbol{k}} \quad (1)$$

where, E_a: activation energy; φ: fuel–air equivalence ratio ($\varphi = 1/\lambda$, where λ is air–fuel equivalence ratio); T and p: ambient temperature [K] and pressure [bar], respectively; R: universal gas constant; m, k and A: adjustable constants. Kinetically, m and A are normally determined as the reaction order and pre-exponential factor, respectively.

In CIEs, Hardenberg and Hase [27] have developed a quite well-known numerical correlation shown in Equation (2). The correlation is based on fuel cetane number, temperature, pressure, engine speed, kinetic parameters (activation energy, apparent activation energy), and some adjustable coefficients.

$$\tau = \frac{3.8 + 0.22\boldsymbol{S_p}}{0.006\boldsymbol{n}}.\boldsymbol{exp}\left[\boldsymbol{E_a}.\left(\frac{1}{\boldsymbol{RT}} - \frac{1}{17190}\right).\left(\frac{21.2}{\boldsymbol{p} - 12.4}\right)^{0.63}\right] \quad (2)$$

where, S_p: mean piston velocity; n: engine speed. $E_a = 618{,}840/(CN + 25)$, where CN is the fuel cetane number. In CIEs, determining kinetic parameters and adjustable constants are very challenging.

The Arrhenius, Hardenberg and Hase correlations have been extended to include the influence of different factors such as (i) fuel type; (ii) fuel properties (e.g. viscosity, density, surface tension, and boiling point); (iii) engine characteristics (e.g. swirl conditions, and compression ratio); and (iv) engine operating conditions (e.g. temperature and pressure at injection, speed, load, stoichiometric mixture conditions) [2–4,28–30]. This leads to quite a few numerical correlations available in the literature. However, ID time computed using those correlations is varying in a wide range [31–34] and this is due to challenges in determining suitable kinetic parameters and adjustable constants as mentioned earlier. This evidence also expresses the complex phenomenon due to physical and chemical processes that are simultaneous occurring toward the auto-ignition event. Further studies therefore are required to provide further knowledge on this issue.

Due to the complex physical and chemical phenomenon happening in the ID_{over} period, scientists have been busy around the world to develop different experiment systems along with numerical and simulation models [3,28] to examine this special period from different angles. Some laboratory tools developed for this purpose are shocktube [35], ignition quality tester and constant volume chambers [4,29], rapid compression machines [3], laboratory atomizers / burners [36], and evaporating systems [23] along with single cylinder engines and multi-cylinder engines [37–39].

Ignition delay was measured as a function of temperature in a constant-volume chamber under simulated diesel engine conditions [30]. A multi-step auto-ignition model was developed by Halstead and co-workers [40] and this model has been further extended to predict diesel spray combustion in [41] to include turbulence and spray atomization sub-models. It is notable that the ID times observed in [30] are in good agreement with the simulated results obtained in [41], the ID time increases almost linearly with the average core temperature during this time lag period.

In present mechanism, auto-ignition is derived in a systematic approach by taking into account the most important elementary reactions' steps (e.g. from unimolecular decomposition, atom abstraction, radical decomposition / isomerization, formation of ketohydroperoxide

and OH, to decomposition of ketohydroperoxide to form oxygenated radical species and OH) [42]. Shocktube is a well-known system to study combustion kinetics purely gas-phase phenomena, it can also be employed to investigate aerosols [18]. Conventional shocktube is proven equipment to test gas-phase chemical kinetics. Fuels used in heat engines, however, mainly in liquid phase. Pre-heating and mixing the fuel and air prior to the ignition chamber is normally done in some shocktubes like the pre-heated one employed in this study. Challenges with shocktube measurements regarding non uniformity in the spatial distribution of aerosols and liquid-phase decomposition of lighter components in practical fuels are reported elsewhere [43]. Aerosol shocktube has been developed to avoid the above difficulties. In this technique, micron size droplets could be directly injected behind the incident shock and reflected shock. The micron droplets quickly transforms to gas-phase and from fuel-air mixture. Methods of prepare and supplied aerosols to this shocktube type can be found in [43]. The reader can be found further information regarding shocktube method, chemical reaction kinetics of biodiesels in some of the best reviews provided in [9,16].Physical and chemical ignition delay times of ultralow sulphur diesel, JP-8, and two synthetic fuels (Sasol IPK and FT-SPK, respectively) have been investigated using an ignition quality tester – IQT (similar to a constant volume chamber) under a temperature range of 778–848 K and a constant pressure of 21 bars [4]. In their study, reacting and non-reacting conditions were established in a constant volume chamber using air and nitrogen, respectively. These two conditions are corresponding to ID_{phys} and ID_{over}. It was found in [4] that ID_{phys} fraction is significant, however, it is noted here that ID_{phys} observed in an IQT is normally longer compared to that in CIEs due to the differences in the injection process, the charge pressure, and turbulence in IQT and CIEs.

ID_{over}, ID_{phys}, and ID_{chem} times of n-heptane and *iso*-octane under IQT conditions were computed using different simulation models [29,44]. It was found that ID_{over} results of shorter ID fuels like n-heptane are significantly sensitive to the selected spray models while longer ID fuels like *iso*-octane are mainly determined by temperature and pressure. The Kelvin Helmholtz – Rayleigh Taylor (KH-RT) model was also suggested as a good model representing fuel spray at all pressure and temperature conditions [44]. The sensitivity mentioned above, again, expresses the complex physical and chemical phenomenon happening toward the auto-ignition event.

A single cylinder engine was adopted in [45] to investigate the influence of fuel chemical profile on ID of pure component fuels. In general, longer ID times were observed for fuels with lower liquid fuel density, kinematic viscosity, and liquid–air surface tension. Longer ID was also observed for component fuels with higher fuel volatility, as measured by boiling point and vapor pressure. Although it is hard to evaluate ID_{phys} and ID_{chem} contributions into ID_{over}, higher boiling point may worsen the fuel evaporating and this ultimately shortens the fuel's ID_{phys}. Experimental data show two regimes of operation: For a Carbon chain length of 12 or greater, there is little variation in ID for the tested fuels. For shorter carbon chain lengths, influence of fuel molecular structure on ID is significant.

A model has been developed in [37] based on a global-mechanism to investigate ID_{phys} and ID_{chem} in a modern diesel engine operating under multi-injection modes (pilot and main). The model is validated with ID_{over} measured in the engine testbed. It is shown that ID_{phys} depends on the charge, fuel thermodynamic conditions, the injector nozzle characteristics and injection pressure. The ID_{chem} has been modelled by means of an Arrhenius-like expression that takes into account the effects of the charge density, total injected fuel quantity, temperature and oxygen concentration evaluated at the end of the physical delay period.

Number of studies on physical and chemical ID is quite limited and the roles of physical and chemical processes on ID_{over} are not quite clear in the literature, according to the authors' knowledge. This study aims to provide further information on the contributions of the physical and chemical processes interact towards the auto-ignition event in CIEs. However, due to the complexity of this issue as mentioned, this work could not come up with a formulation to directly compute physical, chemical, and then overall ignition delay times. This work limits to estimating for time scales for important physical and chemical phenomena.

Data for selected biodiesels having a wide range of molecular structure and fossil diesel are analysed to investigate the relative magnitude of different physical and chemical phenomena influencing auto-ignition event. Within the reason, different fuels manufactured from different feedstock are selected. The fuel auto-ignitability is tested in a cooperative fuel research (CFR) engine and a 6-cylinder engine to measured ID_{over}. Chemical ID is evaluated here using a preheated shocktube in comparison with some other results taken from literature. The preheated shocktube employed in this work can only quantify ID_{chem} under HTC regimes and this along with results taken from other published items for ID_{chem} under NTC and LTC may provide useful information on the chemical processes. Physical ID is examined through evaluating important physical processes including atomization, thermal condition in the combustion chamber that affecting the fuel heating and evaporation. Secondary atomization was experimentally investigated in an air-cross system while evaporation rate was measured for stationary fuel drops located in a PID-controllable furnace.

2. Experiment setup, fuels selection and testing conditions

2.1. Experiment setup

Overall ID times of the selected fuels (see Section 2.2) are measured using two different engines: a cooperative fuel research (CFR) engine and a 6-cylinder engine that are schematically shown in Fig. 1a and 1b, respectively. A preheated shocktube used earlier in [35] is adopted here to measure ID_{chem} under HTC regimes. A fundamental study on drop atomization has also been done using an air-cross system similarly to the one reported in [36] while evaporation rates of the fuels are experimentally examined using a PID-control furnace. This section shows only the specifications of the two engines. Information about other experiment systems adopted in this work will be provided in corresponding sections and/or in relevant refs [35,36]. The observations obtained from the experiment tools allow to quantify the ID_{over} times in CIEs and to evaluate the influence of physical and chemical processes on the ignition lag behavior.

Fig. 1a shows the Cooperative Fuel Research (CFR) engine used in this study and the engine specifications are shown in Table 1. This special tool is a single-cylinder and variable compression ratio (CR) engine initially used for examining fuels but now used worldwide for examining the combustion characteristics of research fuels [46]. Model CFR F-5 engine used in this study is a complete system for measuring the CN of diesel-like fuels, conforming to the ASTM D613 standard. This approach is a standard accepted worldwide for determining the diesel-like fuel auto-ignitability. The capability of varying CR makes the engine special, especially for observing the auto-ignition event of new fuels under different compression temperature (T_i) and pressure (P_i) like biodiesels and their blends with diesel tested in this study. The standardized operating condition of the engine to measure liquid fuel CN [47] is 900 rpm of engine speed and a CR of 13:1. However, the SOI and CR are variable and this as such allows studying the influence of temperature and pressure at SOI on auto-ignitability characteristics. The air-intake temperature is well-controlled at 65 °C for all testing conditions. Further details of this special engine can be found in [48].

The range of data obtained from the CFR F-5 engine is quite useful to isolate the influence of T_i, P_i, and loading conditions on ID_{over}. However, it is notable here that the combustion chamber is more like a constant volume chamber located above the cylinder head and separately from the chamber formed by the cylinder, piston by a small hole located in the piston's centerline [48]. Owing that special combustion chamber, the CFR F-5 engine is quite different from typical compression ignition engines. The injection system equipped in the CFR F-5 engine is

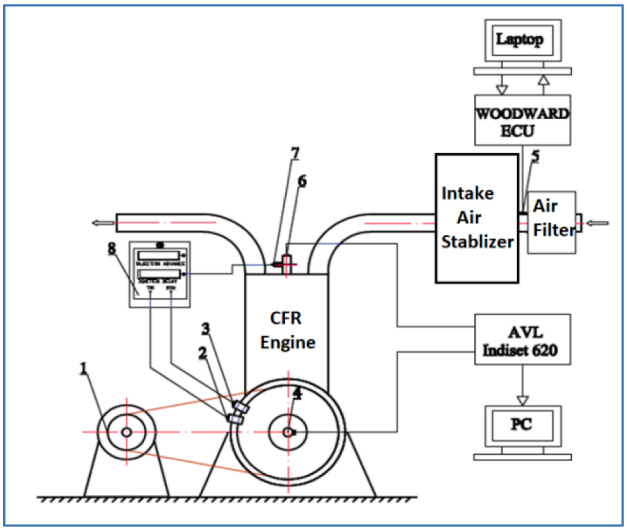

a. Cooperative Fuel Research (CFR-F5) engine

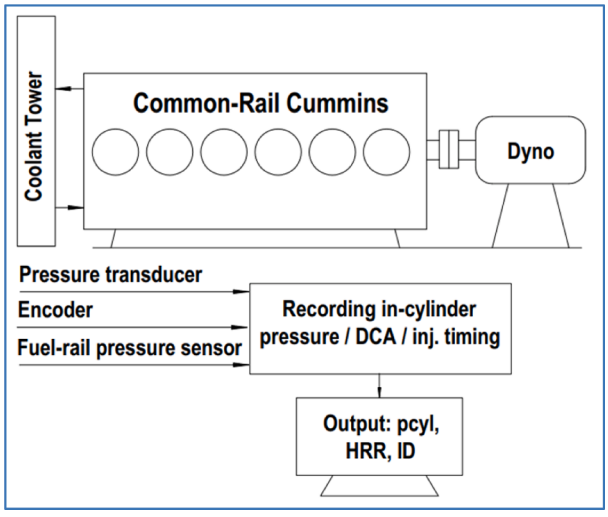

b. 6-cylinder CommonRail engine

Fig. 1. Experiment setup: (a) Schematic of CFR F-5 engine; (b) the 6-cylinder engine.

Table 1
Specifications of the CFR F-5 engine and 6-cylinder engine.

Parameters, [Unit]	CFR F-5	6-cylinder
Speed, [rpm]	900 ± 9	Variable
Injection timing, [DCA BTDC]	8–20 DCA BTDC	TDC ± 2 DCA
Injection type	Mechanical	CommonRail
Injection pressure, [bar]	103.0 ± 0,2	1,000 at 2,000 rpm full load
Compression ratio	8 ÷ 36	17.3
Coolant temperature for injector, [°C]	38 ± 3	N/A
Lubricant pressure, [bar]	1.75 ÷ 2.10	N/A
Lubricant temperature, [°C]	57 ± 8	N/A
Engine coolant temperature, [°C]	100 ± 2	90 ± 2
Intake air temperature, [°C]	65 ± 0.5	20 ± 0.5

mechanically driven and the fuel injection pressure is 103 bars. Injection timing is mechanically controlled and determined using a system to quantify the needle starting lift-up. Due to the characteristics of this CFR F-5 engine, a modern 6-cylinder CommonRail engine was used to further investigate the ID_{over} period. The fuel injection pressure in this multi-cylinder engine can be up to 1,000 bars at 2,000 rpm.

Fig. 1b schematically shows the modern 6-cylinder inline engine testbed while the engine specifications can be found in Table 1. This is a turbocharged, intercooled, CommonRail engine [36,38]. The engine was coupled to an electronically controlled hydraulic dynamometer. A Kistler pressure transducer was used to measure in-cylinder pressure. The fuel injection timing was measured using the signals of fuel rail pressure. Cooling system and intake air temperature are well controlled to remain the engine thermal conditions. This engine testbed has been used in previous studies and further engine specifications could be found in [36]. The 6-cylinder engine was operated in this study under two engine speed conditions (1,500 and 2,000 rpm, respectively) and four engine loading conditions (a quarter, half, three quarters and full load, respectively). Those testing conditions allow examining the influence of fuel properties along with engine operating conditions on ID_{over}. Further specifications can be found in Table 1.

It should be noted here that controlling injection timing and fuel quantity could have influence on results obtained. In the mechanical injection systems, the influence of fuel bulk modulus and therefore compressibility on injection timing is quite clear. A common method used in most of published articles to measure injection timing for mechanical injection system is to use the position of high-pressure throttle lever and this definitely leads to errors in injection timing indicated. Employing the needle lift-up signal in mechanical injection systems (adopted in this CFR engine as noted earlier) is one of approaches to eliminate the above mentioned issue. This problem is, however, not happened to commonrail injection systems thanks to their high injection pressure. Regarding fuel quantity, the amount of fuel volume supplying per one engine cycle could be different due to different viscosity amongst tested fuels. The difference in fuel volume may not be significant but the energy quantity due to different heating values of tested fuels. The latter issue is beyond the research scope of this work, the reader could be directed to refs. [48,49] for further information.

Shocktube employed in this study is a preheated one and has been reported elsewhere [35]. Results obtained in experiment campaign reported in [35] now further explored in this work. Deliver gas used in this shocktube is a varying blending ratio mixture of He and N_2 and supplied to the driver section after evacuating to a pressure below 0.02 Pa. Conditions of temperature and pressure in the shocktube are initiated by combusting $H_2/CO/CO_2/N_2/O_2$/Ar mixture [50]. OH* is measured and used to quantify ID. Details about the shocktube calibration and setup can be found in [50].

An experiment system is developed in this study to examine evaporation rate of stationary drops. Due to different tools used in this study, descriptions of this evaporating experiment system will be shown latter in Fig. 8a where evaporation characteristics are analysed. Briefly, this system includes a heat-controllable furnace, a wire system to carry the tested drop and place it in the measuring probe under desired temperature conditions. A CCD camera along with a light source is setup to observe the drop evaporation process based on the backlit technique reported in [51]. A specialized lens is used to have a partial resolution of 5.5 μm. Images are then processed using an in-house develop Matlab script to output droplet diameter according to the their resident time. This data processing have been proven previously using different validating approaches [36].

2.2. Measurement of ID_{over}

As mentioned, measuring ID_{over} in CIEs could be done by determining SOI and SOC. SOI could be experimentally measured using nozzle lift profile, fuel-line pressure signal, or electronic pulse signal (drive injector, electronic injection systems). SOC could be isolated by observing zero value of heat release rate (HRR) when it changes from negative to positive during the ID period [52]. Fuel injecting and vaporizing cause negative values of appearance HRR prior to the auto-ignition event [52]. Due to fuel auto-ignition, HRR increases

significantly and exceeds zero value, the location that is commonly described as auto-ignition or SOC.

As mentioned earlier, a CFR F-5 engine and a 6-cylinder engine are used to investigate ID_{over} times of biodiesels and their blends with the D. Fig. 2 shows examples of how the auto-ignition event is isolated. Fig. 2a is shown for the CFR engine while Fig. 2b is shown for the 6-cylinder engine.

Fig. 2a provides an example of in-cylinder pressure and corresponding HRR versus degree of crank angle (DCA) obtained for biodiesel PB100 (that will be detailed in Section 2.3) under a CR of 17:1 and two different injection timings (t_{inj} = 10 DCA before top dead center (BTDC) – blue and solid curves & t_{inj} = 14 DCA BTDC – black and dashed curves, respectively). Overall ID is the duration measured between the SOI and SOC. The auto-ignition event is isolated here using the HRR signal. It is noted here that the in-cylinder pressure was measured using a fast response pressure transducer. The in-cylinder pressure is adopted as the main input in the first-law of thermodynamics model provided in [52] to compute HRR. After SOI, the fuel absorbs some heat from the in-cylinder charge for evaporating and this causes negative values of HRR as clearly shown in Fig. 2. SOC is then isolated as the location that the HRR locally becomes zero and reverses direction.

Similar to Fig. 2a, Fig. 2b shows an example of in-cylinder pressure and corresponding HRR obtained for the 6-cylinder engine. This example is shown for biodiesel BF3 that will be detailed in Section 2.3. Using the characteristic of HRR, quantitative information of the ID_{over} obtained from these two engines will be used throughout the paper. It is notable here that SOI in the CFR F-5 engine can be varying in a wider range (e.g. from 8 to 20 DCA BTDC used in this study) while SOI in the 6-cylinder engine is managed by its original ECU. SOI in the 6-cylinder engine (Fig. 2b) is around TDC (±3 DCA) [36].

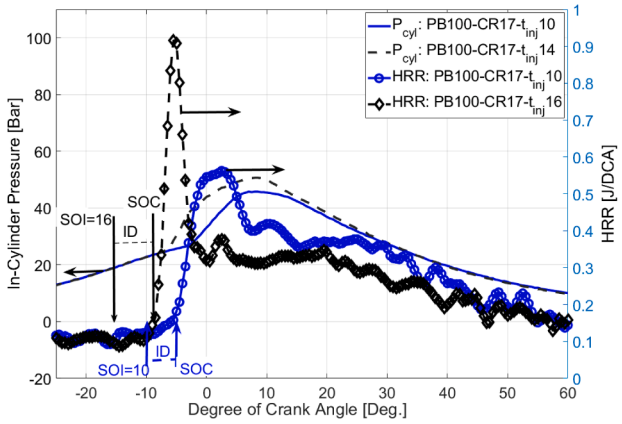

a. Example of ID determining in the CFR F-5 engine

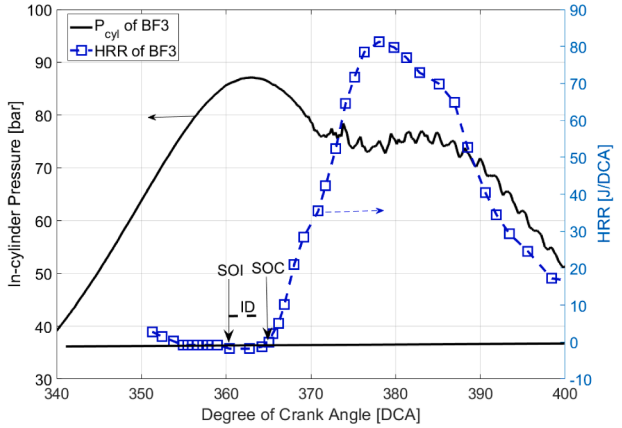

b. Example of ID determining in the 6-cylinder engine

Fig. 2. Example of using pressure & HRR for determining SOC: a. CFR F-5 engine operating with PB100 at tinj = 8 DCA BTDC; b·BF3, 6-cylinder engine at 1,500 rpm, three quarter load condition.

2.3. Fuel selection

Five different biodiesels manufactured from different feedstock and their blends with fossil diesel (D) were selected in this study to examine ID_{over}, ID_{phys}, and ID_{chem}. The first four interesting biodiesels (BF1, BF2, BF3 and BF4, respectively) used earlier in our previous studies [36,53] will be further examined in this study. Palmere and coconut based-oils were the based feedstock to produce BF1 and BF2, respectively; BF3 was produced from pale based-oil while BF4 is a canola based-oil fuel. BF1 and BF2 represent for saturated biodiesels. BF1 has a shorter C chain length while BF2 has a medium C chain length·BF3 and BF4 have long and similar C chain lengths but different saturation degrees·BF3 is partially unsaturated while BF4 is almost fully unsaturated. These characteristics make the fuel group special to study the influence of C chain length and unsaturation degree on atomization, combustion and emission [36]. Further information about the fuels could be found in [36]. The fifth biodiesel, named PB in this study, is a novel biodiesel made from residues of a palm cooking-oil production process by our previous work [49]. Important properties of the selected biodiesels along with fossil diesel are shown in Table 2. Properties of blends of the first four biodiesels and diesel can be found in our previous work [36] while properties of PB blends can be found in [49]. Compositions and important properties of biodiesels shown in Table 2 have been carefully tested using different measurement standards.

It is notable that each experiment in this work may not be conducted to test all of those selected fuels, this is due to the large number of fuels selected as well as experiments and as such the tests were conducted at different time and different laboratories. ID_{over} of PB and its blends were tested in the CFR F-5 engine while ID_{over} of four biodiesels BF1 to BF4

Table 2
Constituents and important properties of biodiesels and D tested in this study.

	BF1	BF2	BF3	BF4	PB	D
CONSTITUENTS' MASS FRACTION						
C8:0	52.16	–	–	–	–	–
C10:0	46.38	0.17	–	–	–	–
C12:0	1.38	47.8	0.1	–	–	–
C14:0	–	18.9	0.06	0.03	–	–
C15:0	–	–	0.03	0.02	–	–
C16:0	–	10.2	21	4.45	28.09	–
C16:1	–	–	–	0.12	–	–
C17:0	–	–	0.06	0	–	–
C18:0	–	2.55	9.47	2.53	9.53	–
C18:1	–	–	–	0.38	43.47	–
C18:1cis	–	18.5	58.7	68.1	–	–
C18:1trans	–	–	–	3.96	–	–
C18:2	–	1.76	9.98	18.7	18.02	–
C20:0	–	0.08	0.3	0.49	–	–
C20:1	–	–	0.24	1.03	–	–
C22:0	–	0.03	0.03	0.17	–	–
Glycerol	0.08	–	–	–	–	–
IMPORTANT PROPERTIES						
	BF1	**BF2**	**BF3**	**BF4**	**PB**	**D**
Average C atoms	9.5	14.8	18.3	18.7	18.94	13.78
Average H atoms	19.7	28.3	35.3	35.3	36.03	26.42
Stoi. AFR, wt	11.12	12.05	12.50	12.48		14.5
Oxygen content, wt%	19.29	13.47	11.14	10.96	10.84	
Flash point, K	60–80	93	101	120	183.5	68.5
Rel. density, at 20 °C, [kg/m^3]	0.877	0.871	0.873	0.879	0.871	0.848
Heating value, MJ/kg	35.35	38.66	39.87	38.07	38.10	43.4
Cetane value	42	69.8	65.4	59	66.9	48.4
Viscosity, [kPa.s]	1.71	3.81	4.32	4.65	6.16	3.2
Surface tension [N/m] *10^3	26.1	28.4	29.9	29.96	24.82 [55]	23

and their blends were tested in the 6-cylinder CommonRail engine. High temperature ID_{chem} of PB was measured using a preheated shocktube similarly to the one used in [35]. Evaporation of PB drops was experimentally measured using a PID controllable furnace developed in this study. Atomization characteristics of BF1 to BF4 were examined in a laboratory atomization system developed earlier in [36].

It is interesting to note from Table 2 that cetane number of biodiesels investigated here is varying in a wide range. This is mainly due to the significant variations in carbon chain length and unsaturation degree of these special fuels. Variations in carbon chain length and unsaturation degree lead to variations in oxygen fraction of the fuels. In general, oxygen available in the fuels could enhance fuel reactivity. However, carbon chain length and number of double bonds (determining unsaturation degree) of fuel molecules also have significant effects on cetane number. Fuels with shorter carbon chain length and / or higher unsaturation degree lower their cetane number [54].

Variations in those biodiesels carbon chain length and unsaturation degree lead to their varying oxygen content. Different from fossil diesel, oxygen content in biodiesels makes them special. Oxygen may leaner the air–fuel ratio in the spray core where the entrance of intake air is quite limited. As can be seen from Table 2 that the oxygen is varying between 10 and 20% amongst these biodiesels and this interesting feature will be investigated in details in Section 3.1.

3. Results and discussion

3.1. Oxygen ratio: An useful indicator of mixture stoichiometry for biodiesels

Oxygen contained in biodiesel molecules is one of the key features making them different from fossil diesel counterpart and as such, in this current study, an approach of using oxygen ratio (OR) given by Mueller et al. [56] will be adopted to represent mixture stoichiometry. Oxygen in the fuel can enhance the fuel auto-ignitability as the oxygen helps to leaner the air–fuel mixture, especially in the auto-ignition zone where the entrance of oxygen from the intake air is limited [17]. Before discussing the results in details, this section will summary Mueller et al.'s approach.

Mueller et al. [56] proposed that the OR and oxygen fuel ratio (OFR) are more appropriate measures of stoichiometry than the standard air to fuel ratio (AFR). At the same air–fuel equivalence ratio (λ), mixtures of oxygenated fuel and air are always leaner compared to mixtures of hydrocarbon fuels and air [17]. The OFR and OR are defined, respectively, as the ratio of total oxygen atoms in the fuels or fuels and oxidizers to the total oxygen atoms required for stoichiometric combustion [17]. Higher oxygen content in a fuel results in a higher OFR, and also a higher difference between the OR and λ. OR can be calculated using Equation (3). It is clear from Equation 6.1 that OR and λ values of D (fuel oxygen contained in D ≈ 0) are the same and higher oxygen content in a fuel results in a higher OFR, and also a higher difference between the OR and λ.

$$OR = \lambda + FO * (1 - \lambda) \quad (3)$$

where, FO is oxygen content by mass in the fuel.

Using AFR data obtained from experiments done the 6-cylinde engine and Equation (3), the correlation of OR and AFR for BF1 to BF4 and D is reported in Fig. 3. This is an example shown for one engine speed of 1,500 rpm but variable engine load fractions (a quarter, half, three quarter and full load). It is clear from Fig. 3 that at the same AFR, D has the lowest OR, followed by BF3, BF4, BF2, and then BF1. This is corresponding with the oxygen fractions in these fuels as shown earlier in Table 2. The OR is now adopted to describe mixture stoichiometry conditions throughout this work.

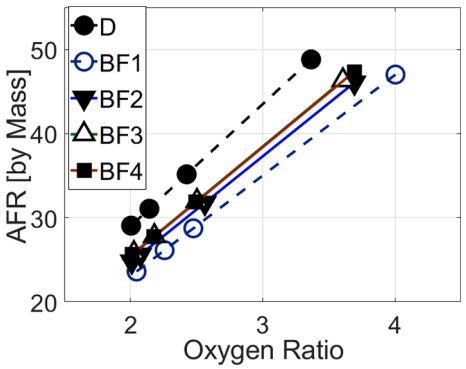

Fig. 3. Air fuel ratio (AFR, by mass) of biodiesels BF1 to BF4 and D versus OR under 1,500 rpm of engine speed and different loading conditions (a quarter, half, three quarter and full load).

3.2. Overall ID in compression ignition engines

3.2.1. Influence of blending ratio on ID_{over}

Fig. 4 shows ID_{over} times of three PB blends (D, PB40 and PB100, respectively) obtained from the CFR F-5 engine under different loading conditions, therefore, different OR. The left column (Fig. 4a & 4c) is shown for CR = 15:1 while the right column (Fig. 4b & 4d) is for CR = 17:1. The top row (Fig. 4a & 4b) is for t_{inj} = 8 DCA BTDC while the bottom row (Fig. 4c & 4d) is for t_{inj} = 16 DCA BTDC. It is noted here that ID_{over} shown here is the time duration in millisecond. This is for a convenience to compare the ID_{over} time observed in engines and the ID_{chem} time measured in a shocktube shown latter on in this work.

It is clearly observed in Fig. 4 that increasing the blending ratio causes reductions in ID_{over} as clearly shown in this figure. This outcome confirms previously reported data [54]. Biodiesels are more reactive compared to the fossil counterparts and the oxygen atoms available in the fuel molecules could be one of the reasons behind this behavior [54]. Diesel-like sprays auto-ignite at a local rich fuel–air zone although the overall mixture is lean and the oxygen available in biodiesel may leaner the local zone to enhance the mixture auto-ignitability.

It is notable that, under similar t_{inj} = 8 DCA BTDC (Fig. 4a and 4b), ID is quite identical regardless CR, however, ID decreases with an increase in CR when t_{inj} = 16 DCA BTDC as clearly shown in Fig. 4c and 4d. It is observed that an increase in CR from 15:1 to 17:1 leads to approximately 15 K increase in the temperature at SOI (at similar t_{inj}). At t_{inj} = 8 DCA BTDC, the temperature at SOI is probably high enough so that the fuel blends are quickly heated, evaporated, mixed with the air and auto-ignited and the influence of temperature difference due to increasing CR in this case is minimal. Under t_{inj} = 8 DCA BTDC, fuel is injected quite close to TDC and this may lead to high cylinder air velocity and turbulence. The high air velocity and turbulence may minimize the impact of compression temperature. At t_{inj} = 16 DCA BTDC, the temperature at SOI is 55–65 K lower compared to that at t_{inj} = 8 DCA BTDC and the fuel blends take longer time to evaporate, mix and get ignited. This is probably the main reason explaining for the longer ID times observed in Fig. 4c and 4d with respect to those shown in Fig. 4a and 4b.

It is quite interesting to note that slopes observed in the reduction trends of ID are quite consistent regardless the CR and blends. In both compression ratios investigated here, when OR increases from 1.4 to 2.2, ID increases by 15% approximately and this is true for both CR = 15:1 and 17:1. It is noted that the intake air temperature is well controlled at 65 °C for the CFR F-5 engine and this means that ID_{over} is determined mainly by the physical and chemical profiles of the testing fuels and the mixture stoichiometry conditions represented here as OR. The fuel profiles will characterize the physical and chemical processes occurring in CIEs which affect the ID_{over} and this will be analyzed throughout this work.

Regarding the correlation between ID_{over} and OR, an increase in OR

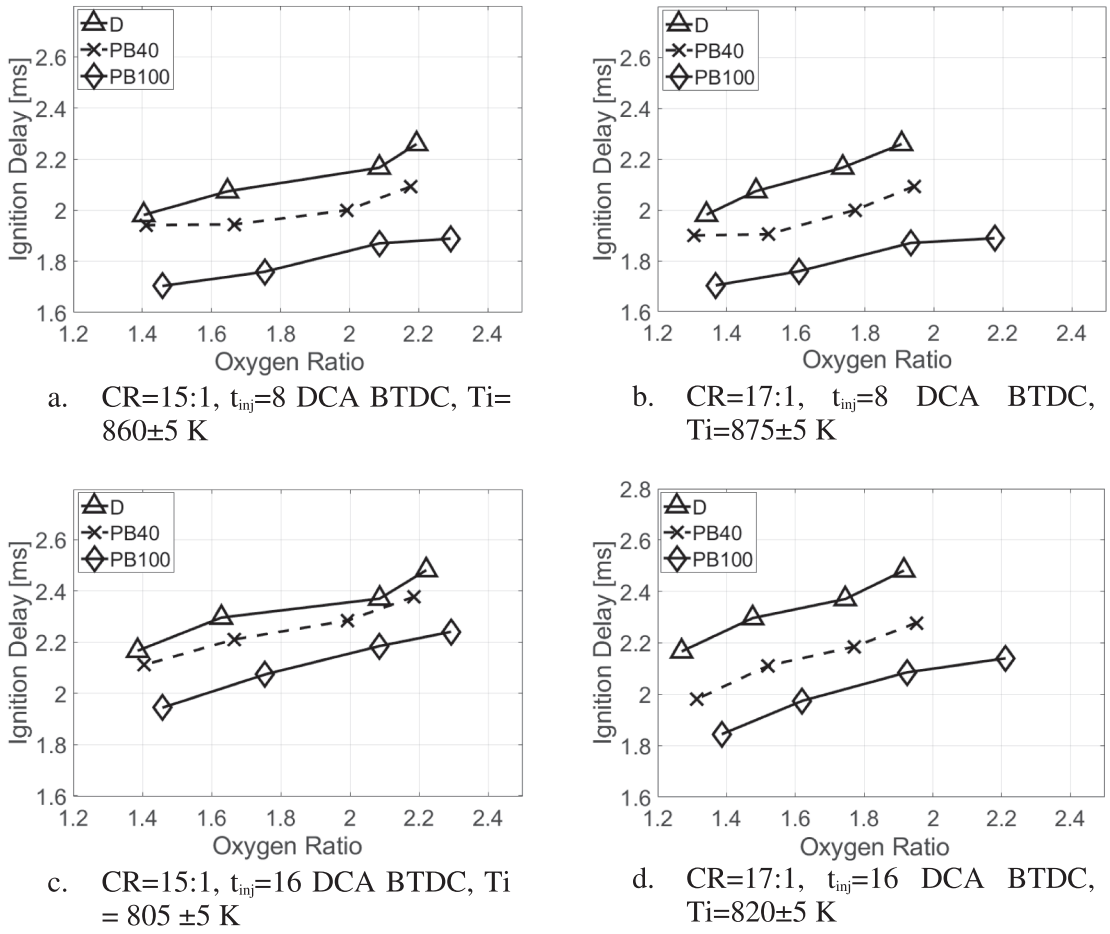

Fig. 4. ID_{over} versus OR measured in the CFR F-5 engine operating with D, PB40 and PB100: a. CR = 15:1, t_{inj} = 8 DCA BTDC; b. CR = 17:1, t_{inj} = 8 DCA BTDC; c. CR = 15:1, t_{inj} = 8 DCA BTDC; and d. CR = 17:1, t_{inj} = 16 DCA BTDC.

(leaner fuel–air stoichiometric mixture or lower engine loading fractions) leads to longer ID_{over} times. Ignition delay is mainly determined by compression temperature and pressure, engine speed and loading conditions. In this CFR F-5 engine, engine speed was fixed at 900 rpm, compression temperature and pressure are identical under similar t_{inj}. Therefore, each curve shown in Fig. 4 indicates the impact of engine loading on ID_{over}. In spark ignition engines, higher engine load may lead to higher air velocity, spray formation and faster mixture formation and this helps to shorten the ID_{over}. Diesel engines work under lean fuel–air mixture and load is regulated by the amount of fuel injection. The bigger amount of fuel injected (lower OR) leads to richer fuel–air mixture and this may be attributable to short ID_{over} in the CFR engine as shown in Fig. 4. Under the same SOI conditions, mixture formation becomes as important as compression temperature and pressure [19].

It is also noted that decreasing OR means increasing fuel injection quantity, it was found earlier that ID_{over} increases with injection quantity in ref. [19] and misfiring occurring from about 2.5 stoichiometric mixture onwards was also found in [19]. If it is assumed that the first

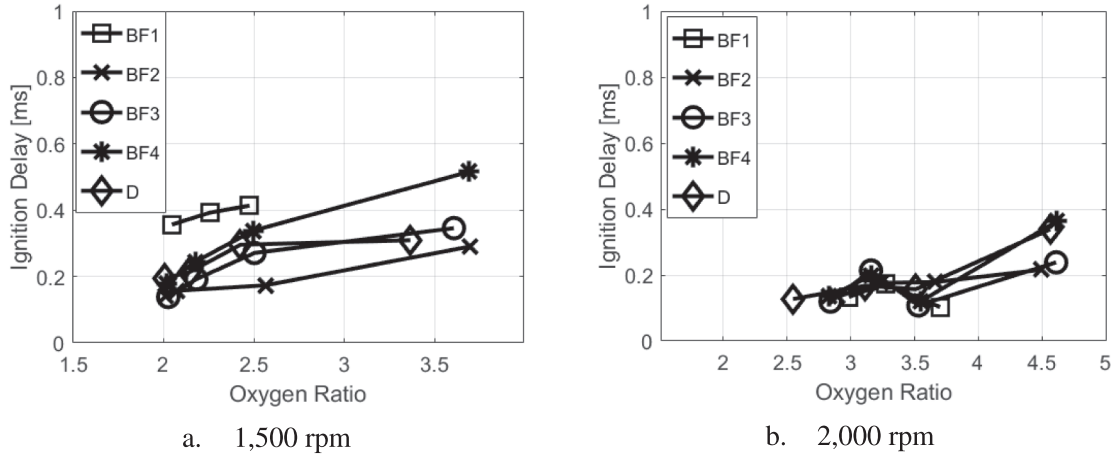

Fig. 5. ID_{over} versus OR measured in the 6-cylinder engine operating with biodiesels BF1 to BF4 and D: a. for 1,500 rpm; b. for 2,000 rpm.

part of the fuel injected will be atomized, vaporized and mixed with the air to from pre-mixture to allow auto-ignition, the influence of subsequently injected fuel on the ID is minimal. However, the quantity injected must be sufficient to form an ignitable mixture and maintain it long enough for the ignition to take place before it is diluted by the air motion to below the inflammable limit [19].

Fig. 5 shows correlations of ID_{over} and OR obtained from the 6-cylinder engine when operating with four different biodiesels BF1 to BF4, respectively, and D. Fig. 5a is shown for 1,500 rpm while Fig. 5b is shown for 2,000 rpm of engine speed.

Fig. 5a clearly shows that ID_{over} time under the engine speed of 1,500 rpm significantly depends on fuel properties. It is clearly shown in Fig. 5 that BF1 with its lowest cetane value (see Table 2) shows its longest ID_{over} time. On the opposite site, BF2 shows its shortest ID due to its highest cetane number. Influence of OR (engine loading conditions) on ID_{over} is similar to observations in the CFR engine as shown earlier in Fig. 4. The reader may find information related to influence of saturated degree and C chain length on combustion characteristics of these fuels from our previous studies [36].

Different from observations from Fig. 5a, when OR < 3.5 as shown in Fig. 5b, ID_{over} times of the biodiesels and D under 2,000 rpm of engine speed are on the same set of windows. The high speed in combination with higher loads (lower OR) help the mixture formed quickly and this may minimize the influence of fuel properties on ID_{over} as observed in Fig. 5b. ID_{over} in this case is probably determined mainly by high temperature chemical processes.

It could be summarized for the relevant discussion provided in this part that ID_{over} depends on fuel types, injection conditions (pressure and temperature), engine speed and load. Higher cetane number fuels normally show their shorter ID_{over}. However, under some testing conditions especially under high engine speed and loading conditions, ID_{over} could be identical regardless fuel types (e.g. the case investigated in Fig. 5b for the 6 cylinder engine). The influence of loading, fuel properties and compression pressure and temperature on ID_{over} will be further investigated in Section 3.2.3.

3.2.2. *Influence of temperature at SOI on ID_{over}*

In this work, injection temperature, T_i, is computed through in-cylinder pressure measured at injection timing. Injection timing in the CFR engine could be adjustable in a wide range as shown in Table 1 and this leads to a wide range of injection temperature in this study. Fig. 6 shows Arrhenius correlations between ID_{over} and $1000/T_i$ for three PB blends (D, PB40 and PB100, respectively) under CR = 15:1 (Fig. 6a) and CR = 17:1 (Fig. 6b). As clearly shown in Fig. 6a and 6b, when $1000/T_i$ excesses 1.2, ID_{over} significantly increases. However, prior to this point (when $1000/T_i < 1.2$ corresponding with $T_i > 833$ K), ID_{over} trend is quite flat even slightly decreases with increasing $1000/T_i$ (e.g. PB40 as shown in Fig. 6a). This opposite ID_{over} trends observed prior and after $1000/T_i = 1.2$ shown in Fig. 6a and 6b might be an evidence for a critical zone separating HTC and NTC regimes in this engine and this will be investigated further in the following part where chemical ID of PB and D observed in a preheated shocktube in this study.

It is shown in Fig. 6a and 6b that, under similar SOI conditions ($1000/T_i$ is similar), increasing CR shortens ID_{over}. Higher CR leads to higher in-cylinder pressure at injection and this will speed up the chemical kinetics and therefore shorten the ID_{over} duration [57]. At $1000/T_i = 1.2$, for example, ID_{over} of PB100 decreases by almost 20% as shown in Fig. 6.

3.3. *Physical and chemical ID*

In this section, the ID_{over} times discussed earlier in the previous sections will be further investigated in terms of ID_{phys} and ID_{chem}. Please note that the work does not aim to measure ID_{phys} and ID_{chem} times but to investigate the influence of physical and chemical processes on the first phase of combustion process. Different from gaseous fuels, combustion of liquid fuels like biodiesels and diesel involves physical processes including liquid penetration, atomization, heating, evaporation and mixing. In this section, two main physical processes including atomization and evaporation will be investigated while chemical processes will be analysed using information related to ID_{chem} obtained under HTC, NTC and LTC regimes. In this study, only HTC ID_{chem} is measured in a preheated shocktube but additional information of ID_{chem} under other conditions taken from literature will be included for a comparison purpose.

3.3.1. *Atomization characteristics of biodiesels and fossil diesel*

Liquid fuel atomization encompasses a number of phenomena including liquid jet primary atomization and secondary atomization processes [58]. Primary atomization initiates the process where the bulk liquid breaks up to form fragments near the liquid surface [21,59], followed by secondary atomization where big fragments having a high relative velocity to the surrounding environment deform and breakup into smaller siblings [21,59].

During the primary atomization process, our previous studies [60] observed that the structures of fuel fragments derived in the primary atomization zone depend on the fuel viscosity [60]. Further downstream of the atomizing zone where breakup has completed (approximately 5 nozzle diameters), the influence of fuel properties is minimal [60]. In this current study, we re-visit secondary atomization characteristics of

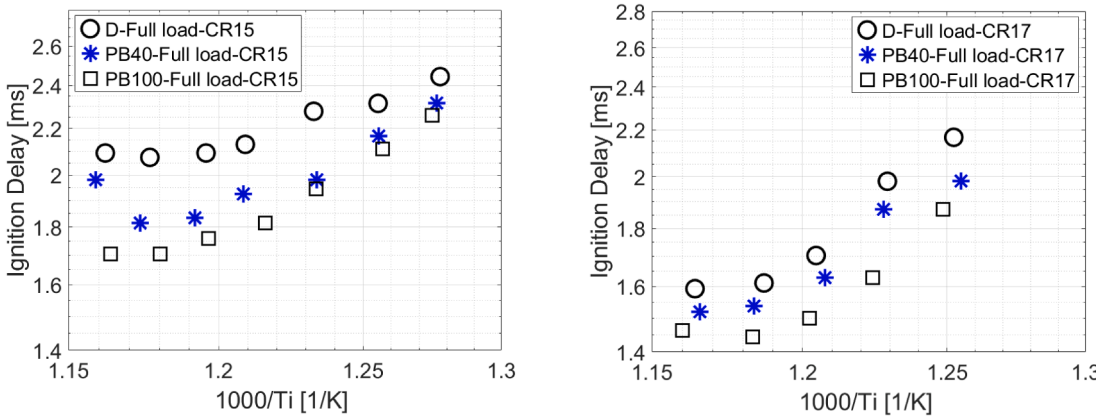

a. CR=15:1 b. CR=17:1

Fig. 6. ID_{over} versus integrated injection temperature, Ti, obtained in the CFR F-5 engine operating with PB blends (D, PB40, and PB100): a. for CR = 15:1; b. CR = 17:1.

droplets in a cross-air flow system similarly to the one used in [36] to evaluate the population of fragments formed in the breakup zone. A backlit imaging technique has been carefully developed [51] and is adopted in this analysis. Fuels investigated here are BF1 to BF4 along with D under different aerodynamics conditions covering a wider range of breakup regimes (from bag, multi-mode, sheet striping, to catastrophic atomization mechanism).

Fig. 7 shows the probability of small drops formed in the downstream location of x/D = 1.7 (where x is the cross-air stream nozzle center line and D = 400 μm is the initial drop diameter used in this study). In this atomization system, x/D = 1.7 is the downstream location where breakup process has completed. The small drops investigated here are fragments having average diameter smaller than 100 μm, almost spherical (aspect ratio < 2:1) and will not breakup again. From left to right, the morphologies of fragments formed in the atomization zone are placed at the top of Fig. 7, corresponding with bag, multi-mode, sheet striping, and catastrophic atomization mechanism. This current work will not investigate the breakup mechanism, relevant information about breakup mechanism and regimes can be found in refs [58]. Fig. 7 focuses on the population of small drops formed in the downstream locations (x/D = 1.7), where breakup process is completed.

It is shown in Fig. 7 that when We < 100, the small drops population depends on fuel types, however, their probability reaches and remains at 80% of the total fragments when We exceeds 200, regardless fuel types. The findings from primary atomization shown previously in [36] and secondary atomization indicate that under high Weber number (e.g. We > 200 in the secondary atomization study) and when breakup has completed (e.g. x/D = 1.7 in the secondary atomization study), the atomization characteristics of biodiesels and D are almost identical.

It is notable that this outcome obtained from the image backlit approach has been confirmed with measurements using a Particle Doppler Anemometry (PDA) system [60]. This also means that the contributions of atomization process of biodiesels and diesel during the delay period are similar although in the breakup zone, structures of fuel fragments may be determined by fuel viscosity. It is noted here that although completed breakup location is identical among the fuels tested here, their relaxation times are different due to their different properties. Relaxation time could be calculated as: $t^*=t/t_c$, where t is residence time; t_c is characteristic breakup time and can be computed as: $t_c = d_o(\rho_l/\rho_g)^{0.5}/U_g$ [61], where U_g is the gas velocity at initial breakup point; ρ_l and ρ_g are fuel and air density, respectively; and d_o is initial fuel droplet diameter. In this study, d_o and ρ_l are the same among the fuels tested, variation in ρ_l is small and as such t_c is mainly determined by gas velocity U_g. To obtain similar We amongst the fuels tested, a fuel with higher viscosity requires higher U_g and this leads to its longer relaxation time, t*.

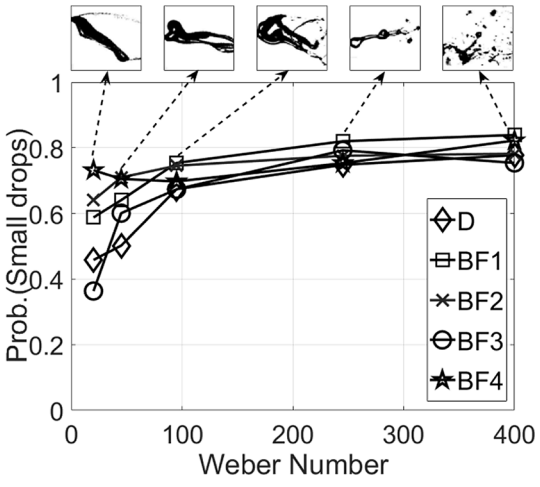

Fig. 7. Morphology and probability of small drops derived from secondary atomization of spherical drops under different aerodynamic.

It should be noted here that quality of atomization / injection is not only attributed by characteristics of fuel fragments formed in the near-field of the nozzle, but also the size and distribution of droplets formed downstream where the atomization process has completed. The drop size and distribution definitely have substantially effects on evaporation, mixing, auto-ignition and combustion characteristics. In our previous report in [62], droplet size and distribution of different fuels (biodiesels including biodiesels investigated in this work, diesel and ethanol) under different flow conditions have been investigated. In this earlier report, size and distribution of droplets were measured using a laser/phase Doppler anemometry. It was found in [62] that the influence of fuel properties on size and distribution of droplets formed downstream (e.g. approximately five nozzle diameter in the atomizer investigated in [62]) is minimal.

3.3.2. *Evaporation characteristics of biodiesels and fossil diesel*

Along with atomization, evaporation is another important phenomenon that has significant impacts on ID. A fundamental experiment system has been developed in this study to measure droplet evaporation rate of D and PB100. The experiment setup is schematically shown in Fig. 8a. This includes a heat-controllable furnace, a wire system to carry the tested drop and place it in the measuring probe under desired temperature conditions. A CCD camera along with a light source is setup to observe the drop evaporation process. The backlit technique is similar to a traditional shadowgraph approach reported in [51]. A specialized lens is used to have a partial resolution of 5.5 μm. A code developed to process the images recorded to output the drop diameter, d, versus time. Fig. 8b shows the correlation between $(d/d_0)^2$ and time for D and PB100, where d_0 is initial drop diameter.

It is clearly shown from Fig. 8b that the evaporation characteristics of these two fuels are quite different. In the first period, PB100 clearly shows its expansion process where $(d/d_0)^2 > 1$ while D's drop size decreases straight away. This could be due to (i) D contains more light components and (ii) D's flash point are lower compared to that of PB100. The expansion of heavy components of D in the first period (heating up process) is probably offset by the fast evaporation rate of lighter components. Volatility of a fuel is inversely proportional to its flash point [54–56]. The flash point of PB is 185.3 °C compared to 68.5 °C of D as reported in Table 2. High volatility enhances fuel evaporation and the formation of an ignitable mixture [9,17] and shortens the physical delay period.

After the heating up process, the rate of evaporation is quite close between these fuels but at the end of the evaporation process D evaporates much slower and this results in the total evaporation times of these fuels are quite identical as shown in Fig. 8. This could be attributed to the fact that D has more heavy constituents with respect to those of PB100. It is obvious that both D and PB100 are multi-component fuels but constituents of D cover a much wider range of C chain length compared to biodiesels [36]. PB100 as shown in Table 2 contains mainly fatty acid methyl esters ranging C16 to C18 while main compound of D is hydrocarbons covering from < C9 to C23 [63]. It is also notable here that the evaporation curves are still above zero at the end of evaporation process for both fuels. This is understandable that the highest boiling point or the boiling of the heaviest component could be higher than the initial temperature tested in this study. For example, the highest boiling point of D is about 760 K [63] while initial temperature used in this study is only 700 K. Studying at higher ambient temperature would provide further scientific information on the evaporation process, however, this is a current limitation of this measuring system and this will be investigated further in the future. It was also found in [64] that contribution of components having a wide range of molecular masses and enthalpies of evaporation of fossil diesel needs to be taken into account, while for biodiesel fuels the main contribution comes from the constituents having a narrow range of molecular masses, boiling points and enthalpies of evaporation.

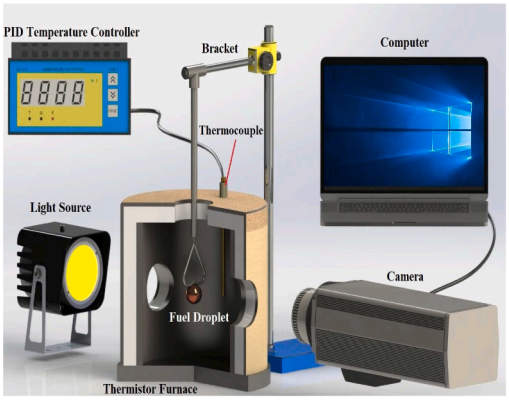

a. Experiment setup

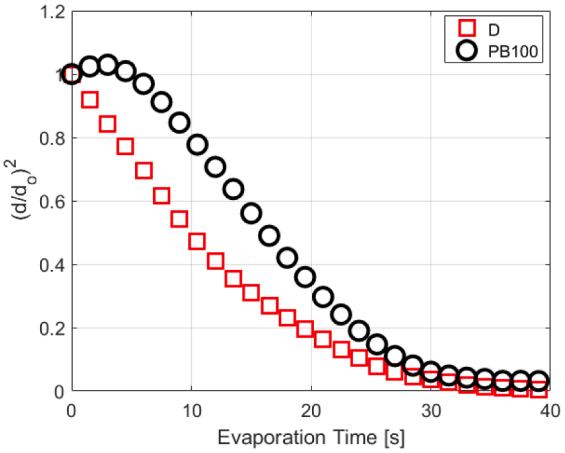

b. Evaporation rate of D and PB100

Fig. 8. a. Droplet evaporation experiment setup and b. Drop evaporation rate of PB100 and D at the condition of: Ti = 700 K; T_0 = 300 K; and d_0 = 1.38 mm.

Ignition delay is mainly affected by the first half of the evaporation process to initialize the premixed combustion process. At the beginning, it is clearly shown that PB100 evaporates much slower compared to D. The slower evaporation rate of PB100 observed here and similar atomization characteristics between D and PB100 mentioned earlier could provide an important point that PB100 has a longer ID_{phys}. However, ID_{over} of PB100 is shorter compared to D. The opposite trend of ID_{phys} and ID_{over} times between PB100 and D observed here suggests a need to investigate ID_{chem} and this will be presented in the flowing section.

It should be noted that the size of drops tested in this work is quite big, much bigger compared to those available in heat engines. An experiment investigates evaporation rates for small drops relevant to heat engines is currently very challenging due to short drop residence time and difficulties in presenting such small drops in hot environment. It was shown in simulation [65,66] that one of important differences between evaporation characteristics of big and small drops is the ratio of Knudsen layer thickness to the drop diameter. Knudsen layer is the layer between drop surface and boundary of vapour zone [66]. The Knudsen layer thickness is independent of drop diameter and as such the Knudsen thickness has a significant impact on evaporation of small drops (e.g. drops having diameter between 10 and 50 um [66]). This is a complex issue and could be a good future work to investigate the influence of small drops of biodiesels with accounting for the impact of Knudsen thickness layer. Nevertheless, from simulation studies available in current literature like [67,68], it is quite consistent that small drops of biodiesels also evaporate slower than those of fossil diesel. The evaporation rate of single drops of rape methyl esters (RME – components of rape-oil based biodiesel) and diesel were experimentally investigated in [68] using a hot-air jet at a temperature condition of 800 K. Diameter of drops generated in the hot-air system is 800 um and the outcome was employed to validate a simulation model developed in [68]. The model is then adopted to compare the influence of drop size and fuel properties on evaporation rate. It was found in [68] that smaller droplets have faster evaporation rate than that of larger droplets ensuring homogenous mixture. 800 um, 400 um and 20 um diameter drops were invested in [68] and found that the RME biodiesel evaporates slower compared to diesel and this is true for the whole range of drop diameter.

3.3.3. Chemical ID

In this current study, PB100 and its blends with D has been tested in a preheated shocktube under an initial temperature conditions between 1180 and 1700 K, OR = 1.96 and pressure = 1.2 bar. The temperature tested here limited in the HTC regime and as such the ID measured here is high temperature ID_{chem}. To provide further information related to the ID_{chem} in NTC and LTC regimes, findings reported earlier in a reflected shocktube [9] are also included in Fig. 9. It is notable that the conditions used in a reflected shocktube [9] is quite different from the preheated shocktube used for testing D and PB in this study. The tests done in [9] under the stoichiometric mixture condition and a pressure condition of 13.5 bars. The tests conducted in [9] and this current work show clearly HTC, NTC and LTC regimes as shown in Fig. 9. NTC regime, being specific to low temperature oxidation processes, is characterized by a zone of temperature in which the overall reaction rate decreases with temperature as shown in Fig. 9 when 1000/Ti between 1.1 and 1.35. NTC phenomena could be considered as a chemical transient regime that allows for continuously transitioning from established LTC to HTC regimes [69]. Qualitatively, from this figure, the regimes having 1000/Ti < 1.1 is corresponding with HTC and 1000/Ti > 1.35 belongs to LTC. It shows that the influence of fuel properties on ID_{chem} is minimal while the influence is significant in NTC and LTC zones. Fuels with higher cetane number cause their shorter ID_{chem} in NTC and LTC regimes [9]. For biodiesels, an increase in carbon chain length and/or a decrease in number of double bonds in the fatty acid esters, biodiesel constituents, leads to shorter ID_{chem}. An increase in carbon chain length and/or a decrease in number of double bonds was also found to increase CN of biodiesels [54]. It is clearly shown in Fig. 9 that ID_{chem} in NTC and LTC zones of methyl Palmitate (16C, 0 double bonds, CN = 86) < methyl Linoleate (18C, 2 double bonds, CN = 38) < methyl Linolinate (18C, 3 double bonds, CN = 23).

It is important to note here that the experiment conditions tested in this study and the conditions tested in the work done by Westbrook et al. [9] is under different pressure and equivalent ratio. The influence of tested conditions on ID is significant. For example, it is stated earlier in [9] that although the region of NTC is very clear but the amount of NTC behavior significantly depends on fuel molecular structure, equivalent ratio and initial pressure. It was shown that at higher initial pressure, the NTC zone shifted toward higher temperature [69]. It was found in [70] ID times exponentially increase when initial pressure decreases, the trend in ID versus temperature however is quite identical and well established in current literature [9,18,70]. Regarding the contribution of equivalent ratio, it was found in [35] that ID increases with an increase in equivalent ratio, however, this impact is fairly minimal. It is shown in Fig. 9 that ID curves obtained in this study is located far from the left side compared to those reported in [9] and, from the discussion provided above, this is mainly attributable to the lower initial pressure (1.2 bar) compared to the pressure tested in [9] (13.5 bar).It was found that the influence of saturated methyl ester group (–COO–CH_3) on combustion is minimal and as such combustion characteristics of saturated methyl esters are extremely identical to saturated n-alkanes with similar number of carbon atoms in their aliphatic main chain [9]. For

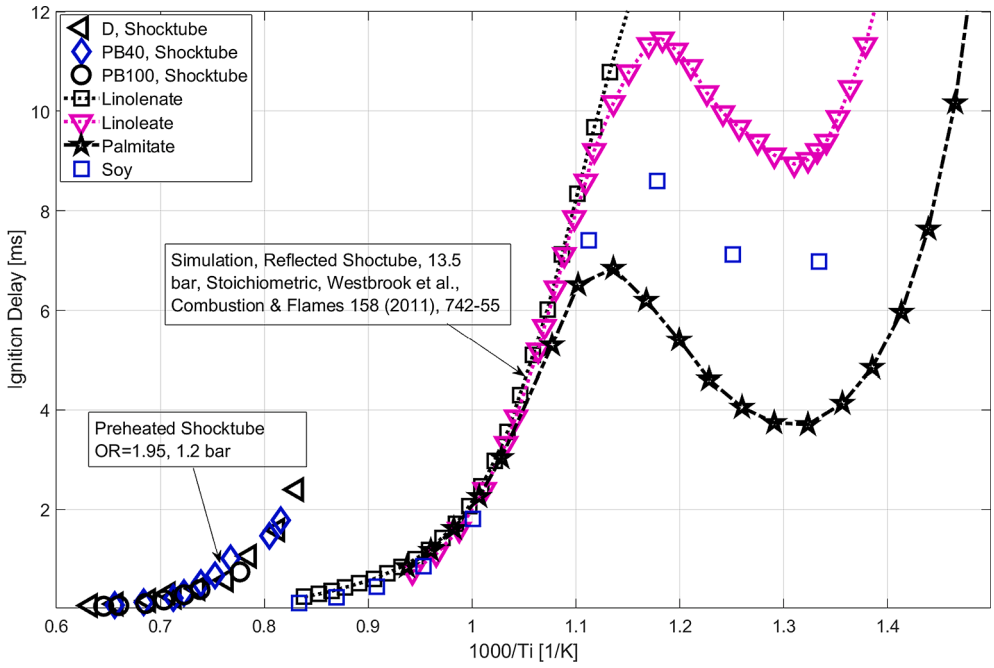

Fig. 9. ID_{chem} time measured using (i) preheated shocktube for D, PB40 and PB100 and (ii) reflected shocktube – like conditions of mono-components of biodiesels including methyl linolenate, methyl linoleate, methyl palmitate and soy methyl ester.

example, the ignition behavior of n-decane ($C_{10}H_{22}$) and methyl decanote ($CH_3(CH_2)_8COOCH_3$) is similar [9]. Chemical kinetic is a challenging topic and the complex structures of fatty acid esters, biodiesel constituents, add further difficulties on this. The reader could be directed to excellent studies [8,9,16,18,69] for current knowledge on biodiesel chemical kinetic mechanism.

From the above discussion, Fig. 10 summarizes the influence of physical and chemical processes on ID_{over} time. Overall ID can be divided into ID_{phys} and ID_{chem} times although physical and chemical processes are not consecutively occurring. This assumption is necessary to eliminate the complexity of this issue. The initial stages prior to the auto-ignition event involves in physical processes (fuel atomization, air entrancement, droplet formation, heating, evaporation, and air–fuel mixing). Chemical reactions, then, takes over and becomes dominant. Although those initial chemical reactions occurring in this delay period, the rate of heat released prior to auto-ignition is fairly small compared to the scale of physical processes.

Atomization of D and biodiesels could be characterized by two important zones: near-field of the nozzle and further downstream. In the near-field zone, morphologies and population of fuel fragments are determined by fuel physical properties, mainly surface tension and viscosity. Biodiesels with higher viscosity compared to fossil diesel show more long ligaments and big un-brocken fragments in the near-field zone. Downstream, however, the influence of fuel properties on the size and distribution of drops derived from atomization is minimal. Evaporation rate of biodiesel drops are higher compared to those of D and this is true for both big and small drops. Compared to D, slower rate of evaporation of biodiesels is probably the main contribution to their

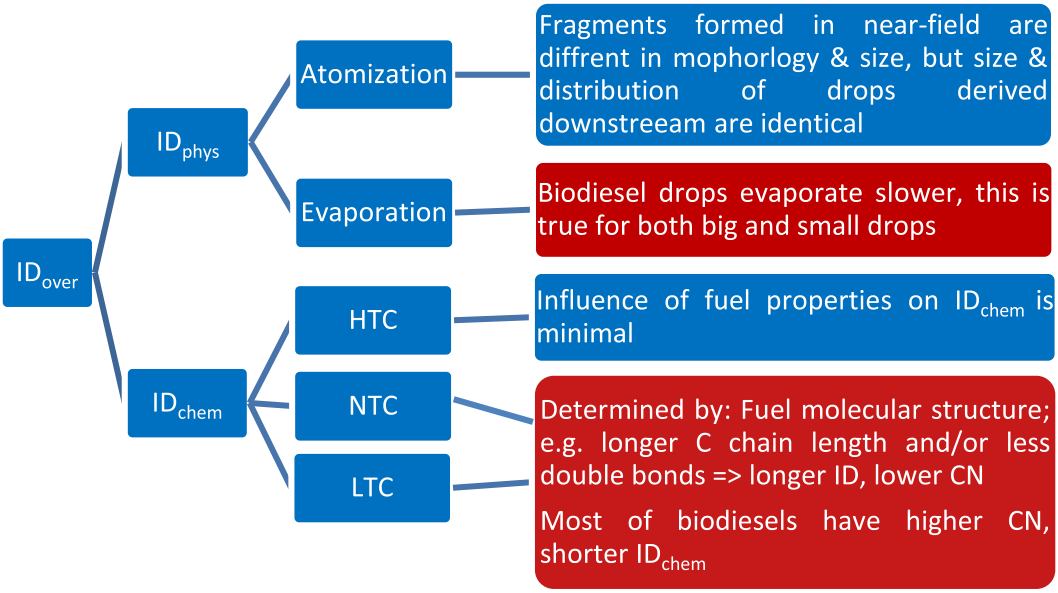

Fig. 10. Flow diagram comparing ID_{over} of biodiesels and fossil diesel accounting for the contribution physical and chemical ignition delay.

longer ID_{phys}.

Chemical processes could be occurring under HTC, NTC or LTC regimes. The difference in ID_{chem} between biodiesels and D are mainly in NTC and LTC regimes. Although kinetic mechanisms between NTC and LTC are certainly different [9,69], fuel molecular structure (e.g. carbon chain length and/or a decrease in number of double bonds in the fatty acid esters, biodiesel constituents) has significant effects on ID_{chem} in those regimes. Common biodiesels have shorter ID_{chem} in NTC and LTC regimes and higher CN compared to D.

In a nutshell, ID_{phys} of biodiesels is longer while ID_{chem} times of most biodiesels under NTC and LTC are shorter. The discussion related to ID_{phys} and ID_{chem} shown above may lead to an interesting statement that shorter ID_{over} of common biodiesels compared to D could be mainly attributed to their shorter ID_{chem} under NTC and LTC regimes.

4. Conclusion

In this context, ID_{over} is the time measured in CIEs and the lag time is caused by physical and chemical processes which lead to physical and chemical ID, respectively. ID_{over} could be understood as the sum of ID_{phys} and ID_{chem} albeit the physical and chemical processes are partly overlapped. This work could not come up with an approach to directly compute physical, chemical, and then overall ignition delay times, it limits to estimating for time scales for important physical and chemical phenomena. The main physical processes include fuel jet atomization, evaporation, and mixing. The chemical ID is attributed to chemical reactions prior to auto-ignition event. The initial chemical reactions could be occurred in HTC, NTC or LTC regimes. In this study, physical and chemical ID periods of biodiesels having a wide range of molecular structure and therefore physical and chemical properties and fossil diesel have been investigated using different research tools. ID_{over} is measured in a CFR F-5 engine along with a 6-cylinder engine. ID_{physic} is evaluated through atomization and evaporation characteristics. ID_{chem} under HTC regimes is characterized using a preheated shocktube and some relevant information of ID_{chem} under LTC, NTC and HTC regimes taken from literature. It can be concluded that:

- Common biodiesels have their higher cetane number compared to that of diesel and this normally leads to their shorter ID_{over}. On some engine operating conditions, like in the commonrail engine under high speed and load fractions investigated in this study, the influence of fuel properties on ID_{over} is minimal. The auto-ignition in this case is mainly determined by chemical processes occurring under high temperature conditions.
- Regarding the physical processes, atomization characteristics (the size and distribution of drops derived downstream where atomization has completed) of biodiesels are identical to that of D. Biodiesels evaporate much slower compared to D especially in the beginning of evaporation process that impacts the formation of initial mixture and as such has significant effects on the auto-ignition event.
- Biodiesels shows their shorter ID_{chem} under NTC and LTC regimes, however, ID_{chem} of biodiesels and diesel is identical under HTC regimes. In overall, compared to diesel, ID_{over} of biodiesels is shorter and this is mainly attributed to their faster chemical reaction rates in NTC and LTC regimes.

CRediT authorship contribution statement

Phuong X. Pham: Conceptualization, Methodology, Validation, Formal analysis, Investigation, Resources, Writing - original draft, Writing - review & editing, Supervision. **Nam V.T. Pham:** Conceptualization, Methodology, Validation, Formal analysis, Investigation, Resources, Writing - review & editing. **Thin V. Pham:** Conceptualization, Methodology, Validation, Formal analysis, Investigation, Resources. **Vu H. Nguyen:** Conceptualization, Methodology, Validation, Formal analysis, Investigation, Resources, Review & editing, Supervision. **Kien T. Nguyen:** Conceptualization, Methodology, Validation, Formal analysis, Investigation, Resources, Writing - review & editing, Supervision.

Declaration of Competing Interest

The authors declare that they have no known competing financial interests or personal relationships that could have appeared to influence the work reported in this paper.

Acknowledgement

This work is financially supported by National Foundation for Science Technology Development (NAFOSTED) under grant number 107.01-2018.310.

References

[1] Lakshminarayanan, P. Aghav, Y.V., Modelling diesel combustion. 2010: Springer Science & Business Media.
[2] Cowart JS, Fischer WP, Hamilton LJ, Caton PA, Sarathy SM, Pitz WJ. An experimental and modeling study investigating the ignition delay in a military diesel engine running hexadecane (cetane) fuel. Int J Engine Res 2013;14(1):57–67.
[3] Lu X, Han D, Huang Z. Fuel design and management for the control of advanced compression-ignition combustion modes. Prog Energy Combust Sci 2011;37(6):741–83.
[4] Zheng, Z., Badawy, T., Henein, N., and Sattler, E., Investigation of physical and chemical delay periods of different fuels in the ignition quality tester. Journal of engineering for gas turbines and power, 2013. 135(6).
[5] Heywood, J.B., Internal combustion engine fundamentals. 2018: McGraw-Hill Education.
[6] Griffiths J, Scott S. Thermokinetic interactions: Fundamentals of spontaneous ignition and cool flames. Prog Energy Combust Sci 1987;13(3):161–97.
[7] Krisman A, Hawkes ER, Talei M, Bhagatwala A, Chen JH. Characterisation of two-stage ignition in diesel engine-relevant thermochemical conditions using direct numerical simulation. Combust Flame 2016;172:326–41.
[8] Mével, R., Sub-Structures in LTC-Affected Detonation.
[9] Westbrook CK, Naik CV, Herbinet O, Pitz WJ, Mehl M, Sarathy SM, et al. Detailed chemical kinetic reaction mechanisms for soy and rapeseed biodiesel fuels. Combust Flame 2011;158(4):742–55.
[10] Aldhaidhawi M, Chiriac R, Badescu V. Ignition delay, combustion and emission characteristics of Diesel engine fueled with rapeseed biodiesel–A literature review. Renew Sustain Energy Rev 2017;73:178–86.
[11] Shahabuddin M, Liaquat A, Masjuki H, Kalam M, Mofijur M. Ignition delay, combustion and emission characteristics of diesel engine fueled with biodiesel. Renew Sustain Energy Rev 2013;21:623–32.
[12] Bittle J, Knight B, Jacobs T. Interesting behavior of biodiesel ignition delay and combustion duration. Energy Fuels 2010;24(8):4166–77.
[13] Bai Y, Wang Y, Wang X. Development of a skeletal mechanism for four-component biodiesel surrogate fuel with PAH. Renewable Energy 2021.
[14] Algayyim SJM, Wandel AP. Macroscopic and microscopic characteristics of biofuel spray (biodiesel and alcohols) in CI engines: A review. Fuel 2021;292:120303.
[15] Xuan T, Sun Z, EL-Seesy AI, Mi Y, Zhong W, He Z, Wang Q, Sun J, El-Zoheiry RM. An optical study on spray and combustion characteristics of ternary hydrogenated catalytic biodiesel/methanol/n-octanol blends; part I: Spray morphology, ignition delay, and flame lift-off length. Fuel 2021;289:119762.
[16] Lai JY, Lin KC, Violi A. Biodiesel combustion: advances in chemical kinetic modeling. Prog Energy Combust Sci 2011;37(1):1–14.
[17] Mueller CJ, Musculus M, Pickett LM, Pitz WJ, Westbrook CK. The oxygen ratio: A fuel-independent measure of mixture stoichiometry (No. UCRL-CONF-201583). Livermore, CA (United States: Lawrence Livermore National Lab.(LLNL; 2003.
[18] Zhang Z, Hu E, Peng C, Meng X, Chen Y, Huang Z. Shock tube measurements and kinetic study of methyl acetate ignition. Energy Fuels 2015;29(4):2719–28.
[19] Lyn, W. and Valdmanis, E., The effects of physical factors on ignition delay. 1968, SAE Technical Paper.
[20] Pham PX, Nguyen KT, Pham TV, Nguyen VH. Biodiesels Manufactured from Different Feedstock: From Fuel Properties to Fuel Atomization and Evaporation. ACS Omega 2020;5(33):20842–53.
[21] Faeth G, Hsiang L-P, Wu P-K. Structure and breakup properties of sprays. Int J Multiph Flow 1995;21:99–127.
[22] Sazhin, S., Droplets and sprays. Vol. 345. 2014: Springer.
[23] Huang X, Wang J, Yuxin W, Qiao X, Ju D, Sun C, et al. Experimental study on evaporation and micro-explosion characteristics of biodiesel/n-propanol blended droplet. Energy 2020:118031.
[24] Wakil ME, Myers P, Uyehara O. Fuel vaporization and ignition lag in diesel combustion. SAE Trans 1956:712–29.
[25] Obert, E.F., Internal combustion engines and air pollution; 1973.
[26] Maroteaux F, Saad C. Diesel engine combustion modeling for hardware in the loop applications: Effects of ignition delay time model. Energy 2013;57:641–52.

[27] Hardenberg H, AnsHase F. An empericalformulaforcomputingthepressurerisedela y of a fuelfromitscetanenumberandfromtherelevantparam eters of directınjectiondieselengines. SAE Paper 1979;790493.
[28] Ra Y, Reitz RD, McFarlane J, Daw CS. Effects of fuel physical properties on diesel engine combustion using diesel and bio-diesel fuels. SAE Int J Fuels Lubr 2009;1 (1):703–18.
[29] Naser N, Sarathy SM, Chung SH. Ignition delay time sensitivity in ignition quality tester (IQT) and its relation to octane sensitivity. Fuel 2018;233:412–9.
[30] Hoskin, D.H., Edwards, C., Siebers, D.L., Ignition delay performance versus composition of model fuels. 1992, SAE Technical Paper.
[31] Assanis DN, Filipi ZS, Fiveland SB, Syrimis M. A predictive ignition delay correlation under steady-state and transient operation of a direct injection diesel engine. J Eng Gas Turbines Power 2003;125(2):450–7.
[32] Rothamer DA, Murphy L. Systematic study of ignition delay for jet fuels and diesel fuel in a heavy-duty diesel engine. Proc Combust Inst 2013;34(2):3021–9.
[33] Rodríguez RP, Sierens R, Verhelst S. Ignition delay in a palm oil and rapeseed oil biodiesel fuelled engine and predictive correlations for the ignition delay period. Fuel 2011;90(2):766–72.
[34] Duong, M.Q., Nguyen, V.H., and Pham, P.X. Development of Empirical Correlations for Ignition Delay in a Single Cylinder Engine Fueled with Diesel/ Biodiesel Blends. in 2019 International Conference on System Science and Engineering (ICSSE); 2019. IEEE.
[35] Hoang VN, Thi LD. Experimental study of the ignition delay of diesel/biodiesel blends using a shock tube. Biosyst Eng 2015;134:1–7.
[36] Pham, X.P., Influences of molecular profiles of biodiesels on atomization, combustion and emission characteristics; 2014.
[37] Finesso R, Spessa E. Ignition delay prediction of multiple injections in diesel engines. Fuel 2014;119:170–90.
[38] Odibi C, Babaie M, Zare A, Nabi MN, Bodisco TA, Brown RJ. Exergy analysis of a diesel engine with waste cooking biodiesel and triacetin. Energy Convers Manage 2019;198:111912.
[39] Jayabal R, Thangavelu L, Velu C. Experimental investigation on the effect of ignition enhancers in the blends of sapota biodiesel/diesel blends on a CRDi engine. Energy Fuels 2019;33(12):12431–40.
[40] Halstead M, Kirsch L, Prothero A, Quinn C. A mathematical model for hydrocarbon autoignition at high pressures. Proceed Roy Soc London A Mathemat Phys Sci 1975;346(1647):515–38.
[41] Kong, S.-C. Reitz, R.D., Multidimensional modeling of diesel ignition and combustion using a multistep kinetics model; 1993.
[42] Bikas, G., Kinetic mechanism for hydrocarbon ignition. 2001, Bibliothek der RWTH Aachen.
[43] Haylett D, Davidson D, Hanson R. Second-generation aerosol shock tube: an improved design. Shock Waves 2012;22(6):483–93.
[44] Jaasim M, Elhagrasy A, Sarathy M, Chung S-H, Im HG. Auto-ignition and Spray Characteristics of n-heptane and iso-octane Fuels in Ignition Quality Tester. SAE Technical Paper 2018–01-0299, 2018..
[45] Caton, P.A., Hamilton, L.J., Cowart, J.S., Understanding ignition delay effects with pure component fuels in a single-cylinder diesel engine. J Eng Gas Turb Power; 2011. 133(3).
[46] Montoya JPG, Diaz GJA, Arrieta AAA. Effect of equivalence ratio on knocking tendency in spark ignition engines fueled with fuel blends of biogas, natural gas, propane and hydrogen. Int J Hydrogen Energy 2018;43(51):23041–9.
[47] ASTM, Standard test method for cetane number of diesel fuel oil. 2010, ASTM International West Conshohocken, PA.
[48] Nguyen VH, Duong MQ, Nguyen KT, Pham TV, Pham PX. An Extensive Analysis of Biodiesel Blend Combustion Characteristics under a Wide-Range of Thermal Conditions of a Cooperative Fuel Research Engine. Sustainability 2020;12(18): 7666.
[49] Nguyen VH, Pham PX. Biodiesels: Oxidizing enhancers to improve CI engine performance and emission quality. Fuel 2015;154:293–300.
[50] Thi LD, Zhang Y, Fu J, Huang Z, Zhang Y. Study on ignition delay of multi-component syngas using shock tube. Canad J Chem Eng 2014;92(5):861–70.
[51] Pham PX, Kourmatzis A, Masri AR. Simultaneous volume-velocity measurements in the near field of atomizing sprays. Meas Sci Technol 2017;28(11):115203.
[52] John, B., Heywood internal combustion engine fndamentals. 1988, McGraw-Hill Book Company.
[53] Pham P, Bodisco TA, Stevanovic S, Rahman M, Wang H, Ristovski Z, et al. Engine performance characteristics for biodiesels of different degrees of saturation and carbon chain lengths. SAE Int J Fuels Lubr 2013;6(1):188–98.
[54] Knothe, G., Krahl, J., Van Gerpen, J., The biodiesel handbook; 2015: Elsevier.
[55] Allen CA, Watts KC, Ackman RG. Predicting the surface tension of biodiesel fuels from their fatty acid composition. J Am Oil Chem Soc 1999;76(3):317–23.
[56] Mueller CJ, Pitz WJ, Pickett LM, Martin GC, Siebers DL, Westbrook CK. Effects of oxygenates on soot processes in DI diesel engines: experiments and numerical simulations. SAE Trans 2003:964–82.
[57] KHAN QS, Baek SW, Ghassemi H. On the autoignition and combustion characteristics of kerosene droplets at elevated pressure and temperature. Combust Sci Technol 2007;179(12):2437–51.
[58] Hsiang L-P, Faeth GM. Near-limit drop deformation and secondary breakup. Int J Multiph Flow 1992;18(5):635–52.
[59] Dumouchel C. On the experimental investigation on primary atomization of liquid streams. Exp Fluids 2008;45(3):371–422.
[60] Kourmatzis A, Pham PX, Masri AR. Air assisted atomization and spray density characterization of ethanol and a range of biodiesels. Fuel 2013;108:758–70.
[61] Varga CM, Lasheras JC, Hopfinger EJ. Initial breakup of a small-diameter liquid jet by a high-speed gas stream. J Fluid Mech 2003;497:405–34.
[62] Kourmatzis A, Pham PX, Masri AR. Characterization of atomization and combustion in moderately dense turbulent spray flames. Combust Flame 2015;162 (4):978–96.
[63] Chevron, G.M., Diesel Fuels Technical Review; 2007, Freighttiner.
[64] Sazhin S, Al Qubeissi M, Kolodnytska R, Elwardany A, Nasiri R, Heikal M. Modelling of biodiesel fuel droplet heating and evaporation. Fuel 2014;115: 559–72.
[65] Miller R, Harstad K, Bellan J. Evaluation of equilibrium and non-equilibrium evaporation models for many-droplet gas-liquid flow simulations. Int J Multiph Flow 1998;24(6):1025–55.
[66] Zudin, Y.B., Zudin, Non-equilibrium evaporation and condensation processes. 2019: Springer.
[67] Al Qubeissi M, Sazhin S, Crua C, Turner J, Heikal M. Modelling of biodiesel fuel droplet heating and evaporation: Effects of fuel composition. Fuel 2015;154: 308–18.
[68] Saha A, Kumar R, Basu S. Infrared thermography and numerical study of vaporization characteristics of pure and blended bio-fuel droplets. Int J Heat Mass Transf 2010;53(19–20):3862–73.
[69] Coniglio L, Bennadji H, Glaude PA, Herbinet O, Billaud F. Combustion chemical kinetics of biodiesel and related compounds (methyl and ethyl esters): Experiments and modeling–Advances and future refinements. Prog Energy Combust Sci 2013;39 (4):340–82.
[70] Lapuerta M, Hernández JJ, Fernández-Rodríguez D, Cova-Bonillo A. Autoignition of blends of n-butanol and ethanol with diesel or biodiesel fuels in a constant-volume combustion chamber. Energy 2017;118:613–21.